^{51}V NMR Study of a C15 Laves Phase Compound HfV_2

Yutaka Kishimoto and Takashi Ohno

Department of Physics, Faculty of Engineering, Tokushima University, Tokushima 770-8506, Japan

Reprint requests to Y. K.

Z. Naturforsch. **57a,** 513–517 (2002); received June 25, 2002

Presented at the XVIth International Symposium on Nuclear Quadrupole Interactions, Hiroshima, Japan, September 9–14, 2001.

We analyzed the K-χ plot in order to investigate the change in the electronic state in the C15 Laves phase compound HfV_2 at the lattice transformation temperature T_L (~ 120 K). We could obtain $K_{3d\ orb}$, $\chi_{3d\ orb}$ and $\chi_{5d\ orb} + (2/3)\ \chi_{Pauli} + \chi_{dia}$, which are consistent with those reported in our previous paper, and discussed the changes in density of states of the V 3d and 4s electrons at T_L.

For the superconducting state we discussed the d wave Anderson-Brinkman-Morel (ABM) type energy gap in which the gap is anisotropic and vanishes at points on the Fermi surface.

Key words: HfV_2; Anisotropic Energy Gap; Knight Shift; Spin-lattice Relaxation Rate; Magnetic Susceptibility.

1. Introduction

For the heavy-Fermion-superconductors and the copper-oxide-high T_c-superconductors it is well known that the T^3 law appears in the temperature dependence of spin-lattice-relaxation-rate $1/T_1$ measured by NMR in the superconducting state, reflecting the anisotropic energy gap. The gap anisotropy in these materials originates from the strong electron correlation. So not only the superconducting state but also the normal state is fascinating.

In the newly discovered superconductor MgB_2 ($T_c = 39$ K), $1/T_1$ of ^{11}B has a small coherence peak just below T_c and obeys the exponential law with $2\Delta(0)/k_BT_c \sim 5$ well below T_c [1]. This large gap suggestes a strong coupling, but MgB_2 is considered to be an s wave superconductor. In superconductors such as Sr_2RuO_4, $CeCoIn_5$, $CeIrIn_5$ and $CeRhIn_5$, the anisotropy in the energy gap has also been discussed in connection with the mechanism of superconductivity. In Sr_2RuO_4 ($T_c \sim 1.5$ K), $1/T_1$ of ^{101}Ru exhibits a sharp decrease without a coherence peak just below T_c and shows a T^3 behavior down to 0.15 K [2], which is consistent with the line-node gap model. In $CeCoIn_5$, $CeIrIn_5$ and $CeRhIn_5$, the T^3 dependence of $1/T_1$ of ^{115}In is also reported well below T_c [3, 4]. The ^{59}Co and ^{115}In Knight shift in $CeCoIn_5$ decreases below T_c, and the Cooper pair is considered to be a spin singlet.

Even in the conventional superconductors, such as the A15 compounds V_3Si and Nb_3Sn and a C15 Laves phase compound HfV_2, the anisotropy in the superconducting energy gap is interesting. In these materials the Hamiltonian of a two level system, which is formed by the strong electron-phonon coupling, is proven to be equal to that of the Kondo system with a 1/2 spin impurity [5, 6]. The periodic two level system corresponds to the dense Kondo (heavy Fermion) system. This strong electron-phonon coupling also induces the lattice transformation. We have measured the ^{51}V NMR in HfV_2 and reported that $1/T_1$ shows a T^5 dependence and the Knight shift K due to the 3d spin vanishes completely well below T_c (= 9.2 K) [7, 8]. In the normal state, K depends linearly on the susceptibility χ above and below the lattice transformation temperature T_L (~ 120 K). The hyperfine field is obtained as -250 kOe/μ_B and -72 kOe/μ_B above and below T_L, respectively. This change is due to the change on the electronic state induced by the lattice transformation.

In this paper we analyze the K-χ plot in the normal state and compare the result with another analysis reported in [7]. In the superconducting state we discuss the d wave Anderson-Brinkman-Morel (ABM) type energy gap, in which the gap vanishes at points on the Fermi surface.

2. K-χ plot

Figure 1 (a) shows the temperature dependence of K in the normal state [7]. The decrease in K with decreasing temperature is ascribed to the increase in the core-

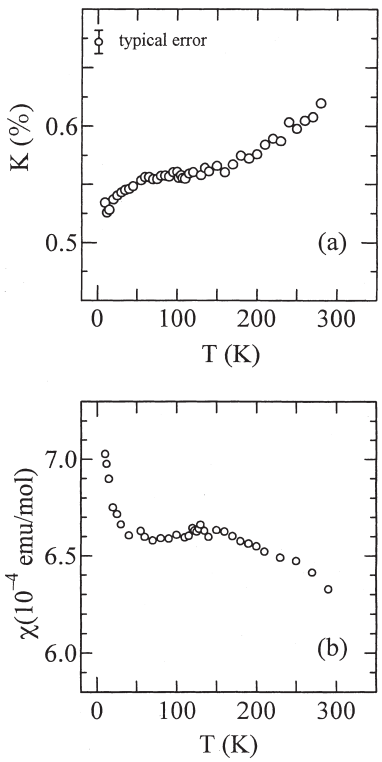

Fig. 1. Temperature dependence of (a) ^{51}V Knight shift K and (b) magnetic susceptibility χ in the normal state.

polarization due to the V 3d spin associated with the increase in χ, whose temperature dependence is shown in Fig. 1 (b). χ and K are written as [9]

$$\chi = \chi_{3d}(T) + \chi_{3d\,orb} + \frac{2}{3}\chi_{4s} + \chi_{5d}(T) + \chi_{5d\,orb} + \frac{2}{3}\chi_{Pauli} + \chi_{dia}\,, \quad (1)$$

$$K = K_{3d}(T) + K_{3d\,orb} + K_{4s}\,, \quad (2)$$

where $\chi_{3d}(T)$, χ_{4s}, $\chi_{3d\,orb}$ and χ_{dia} are the spin susceptibilities due to V 3d and 4s electrons, the orbital susceptibility due to V 3d electrons and the diamagnetic susceptibility due to the V and Hf core electrons, respectively. $\chi_{5d}(T)$ and $\chi_{5d\,orb}$ are the spin susceptibility and the oribital susceptibility due to Hf 5d electrons, respectively. χ_{Pauli} is the spin susceptibility due to V 3p, Hf 5p, Hf 6s and other electrons. $\chi_{dia} \sim -4.6 \times 10^{-5}$ emu/mol is given by Gupta [10]. $K_{3d}(T)$, $K_{3d\,orb}$ and K_{4s} are proportional to $\chi_{3d}(T)$, $\chi_{3d\,orb}$ and χ_{4s}, respectively and written as

$$K_i = H_{hf}^{i}\,\frac{\chi_i}{N_A\,\mu_B}\;(i = 3d, 3d\,orb, 4s), \quad (3)$$

where H_{hf}^{i} is the corresponding hyperfine field and N_A Avogadro's number. $H_{hf}^{3d\,orb} = 216$ kOe/μ_B is given from the formula, $H_{hf}^{3d\,orb} = 2\,\mu_B\,\langle r^{-3}\rangle \cdot 0.75$ and $\langle r^{-3}\rangle = 1.56 \cdot 10^{25}$ cm^{-3}, calculated for a V atom with $[3d]^4$ configuration by Freeman and Watson [11]. We assume that $\chi_{5d}(T)$ is negligibly small because the density of states (DOS) $N_{5d}(\varepsilon_F)$ at the Fermi level due to Hf 5d electrons is only one tenth of $N_{3d}(\varepsilon_F)$ due to V 3d electrons according to a band calculation [12].

In the previous paper we estimated $N_{3d}(\varepsilon_F)$, $N_{4s}(\varepsilon_F)$ due to V 4s electrons, $K_{3d\,orb}$, K_{4s}, $\chi_{3d\,orb}$ and $\chi_{5d\,orb}$ + (2/3) χ_{Pauli} + χ_{dia} in the following way [7]. In the low-temperature region we assumed the Korringa relation between the relaxation rate $1/T_1T$ and the Knight shift K due to V 3d and 4s electrons. The least-squares fit to the measured data of $1/T_1T$ and K yields $K_{3d\,orb}$, K_{4s} and $N_{4s}(\varepsilon_F)$. $\chi_{3d\,orb}$ is estimated from $K_{3d\,orb}$. To estimate $N_{3d}(\varepsilon_F)$, we used $\chi = 7.0 \cdot 10^{-4}$ emu/mol observed at 10 K. The total spin susceptibility and the total DOS $N(\varepsilon_F)$ are estimated from the observed value of the electronic specific heat coefficient γ. In the high-temperature region, the temperature dependence of $K_{3d}(T)$ and $(1/T_1T)_{3d}$ due to V 3d electrons is discussed, based on the narrow band models, *Simple Lorentzian model* and *Two-peak model*. We fit the calculated K and $1/T_1T$ to the observed temperature dependence of them simultaneously by the least-squares method in order to determine $N_{3d}(\varepsilon_F)$, $K_{3d\,orb}$, K_{4s}, and $(1/T_1T)_{4s}$ due to V 4s electrons. The estimated DOS, K and χ are shown in Table 1.

K is plotted against χ with the temperature as an implicit parameter in Fig. 2 (K-χ plot). As shown in the inset, K depends linearly on χ in both temperature ranges, 130–280 K and 10–90 K. From the slopes of the solid and broken lines in Fig. 2, the hyperfine field $H_{hf}^{3d} = -250$ kOe/μ_B (high-temperature region) and -72 kOe/μ_B (low-temperature region) are obtained. This change in H_{hf}^{3d} is too large to be attributed to a change in the core-polarization due to the V 3d spin. Since the magnitude of H_{hf}^{4s} is one order of magnitude larger than H_{hf}^{3d}, a strong 4s–3d mixing sometimes reduces the magnitude of the hyperfine field of transition elements. We believe that the above decrease in the magnitude of the hyperfine field originates from the 4s–3d mixing induced by the lattice transformation. The fraction of $N_{3d}(\varepsilon_F)$ which has 4s character is estimated to be about 16% to explain this decrease.

χ_{4s} and K_{4s} are negligibly small because $N_{4s}(\varepsilon_F)$ is negligibly small [7, 12]. We introduce the parameters $x = \chi_{5d\,orb}/\chi_{3d\,orb}$ and $y = N_{3d}(\varepsilon_F)/N(\varepsilon_F)$. We write

Table 1. Density of states, Knight shift and magnetic susceptibility estimated in [7].

	$N(\varepsilon_F)$	$N_{3d}(\varepsilon_F)$	$N_{4s}(\varepsilon_F)$	$N_{3d}(\varepsilon_F)/N(\varepsilon_F)$	$K_{3d\,orb}$	$\chi_{3d\,orb}$	$\chi_{5d\,orb} + 2/3\,\chi_{Pauli} + \chi_{dia}$
	(states (eV)$^{-1}$/V spin)				(%)	(10^{-4} emu/mol)	
Low-temperature region	2.36	1.60	1.3×10^{-3}	0.68	0.66	3.4	1.5
High-temperature region							
Simple Lorentzian model	<1.84*	1.22	4.5×10^{-2}	>0.66*	0.85	4.4	0.80
Two-peak model	<0.89*	0.66	3.8×10^{-2}	>0.73*	0.90	4.7	0.31
Band calculation**	0.91	0.64	–	0.70			

* $\chi_{dia} + \chi_{5d\,orb} > 0$ is assumed, though $\chi_{5d\,orb}$ is not known; ** Reference [12].

Table 2. $K_{3d\,orb}$, $\chi_{3d\,orb}$ and $\chi_{5d\,orb} + (2/3)\,\chi_{Pauli} + \chi_{dia}$ estimated from the K-χ plot for some values of x (= $\chi_{5d\,orb}/\chi_{3d\,orb}$) and y (= $N_{3d}(\varepsilon_F)/N(\varepsilon_F)$).

	$N(\varepsilon_F)$	$\chi_{5d\,orb}/\chi_{3d\,orb}$	$N_{3d}(\varepsilon_F)/N(\varepsilon_F)$	$K_{3d\,orb}$	$\chi_{3d\,orb}$	$\chi_{5d\,orb} + (2/3)\,\chi_{Pauli} + \chi_{dia}$
	(states (eV)$^{-1}$/V spin)			(%)	(10^{-4} emu/mol)	
Low temperature region	2.36	0.5	0.53	0.63	3.2	2.1
	2.36	0.39	0.68	0.66	3.4	1.5
High temperature region	1.84	0.2	0.7	0.84	4.4	0.89
	1.84	0.2	0.8	0.86	4.5	0.75
	0.91	0.2	0.7	0.86	4.5	0.68
	0.91	0.2	0.8	0.87	4.5	0.61

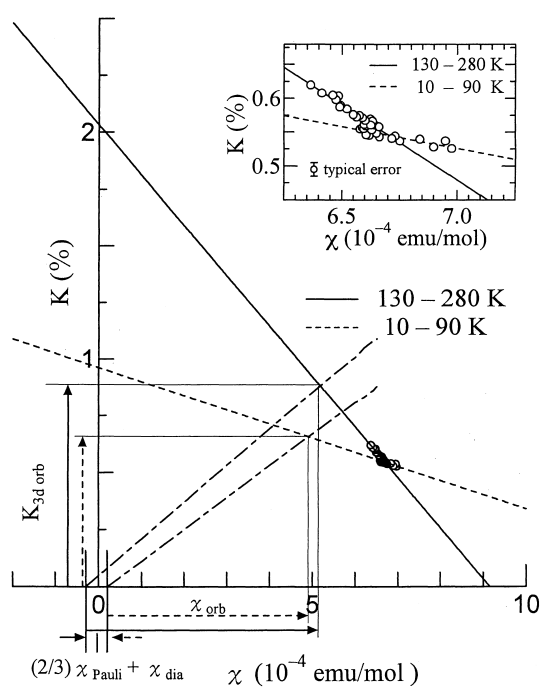

Fig. 2. K-χ plot. Broken and solid lines show the linear fit below and above the lattice transformation temperature T_L (~ 120 K), respectively. The parameters, $K_{3d\,orb}$, χ_{orb} and 2/3 χ_{Pauli} + χ_{dia} for $x = 0.39$ and $y = 0.68$ in the low-temperature region, and those for $x = 0.2$, $y = 0.8$ and $N(\varepsilon_F) = 1.84$ states (eV)$^{-1}$/V spin in the high temperature region are illustrated by the broken and solid lines, respectively. An enlarged plot is also shown.

$\chi_{3d\,orb} + \chi_{5d\,orb} = (1 + x)\,\chi_{3d\,orb} = \chi_{orb}$. χ_{Pauli} is obtained from $\chi_{Pauli} = 2\,\mu_B^2\,(1 - y)\,N(\varepsilon_F)$. In the low-temperature region, using these χ_{orb}, χ_{Pauli}, $\chi_{dia} = -4.6 \cdot 10^{-5}$ emu/mol and $\chi = 7.0 \cdot 10^{-4}$ emu/mol measured at 10 K, we can estimate $\chi_{3d}(T = 0)$. From $\chi_{3d}(0) = 2\,\mu_B^2\,N_{3d}(\varepsilon_F)$ we can estimate $N_{3d}(\varepsilon_F)$ as a function of x and y. From $N_{3d}(\varepsilon_F)/N(\varepsilon_F) = y$ we get the relation $1.3\,(1 - x) = (1 + 0.51\,x)\,y$. Here, we used $N(\varepsilon_F) = 2.36$ states (eV)$^{-1}$/V spin estimated from the electronic specific heat coefficient γ [7, 8]. From the condition $0 < y < 1$, $0.18 < x < 1$. When $x = 1$, y becomes too small ($y = 0$), while for $x = 0.2$, y becomes too large ($y = 0.97$). The suitable value of x is considered to be about 0.5. In the previous paper we estimated $y = 0.68$ [7], and then $x = 0.39$. In Table 2, $K_{3d\,orb}$, $\chi_{3d\,orb}$ and $\chi_{5d\,orb} + (2/3)\,\chi_{Pauli} + \chi_{dia}$, estimated for $x = 0.5$ and $x = 0.39$, are given. $K_{3d\,orb} = 0.66\%$, $\chi_{3d\,orb} = 3.4 \cdot 10^{-4}$ emu/mol and $\chi_{5d\,orb} + (2/3)\,\chi_{Pauli} + \chi_{dia} = 1.5 \cdot 10^{-4}$ emu/mol estimated for $x = 0.39$ agree with those obtained in the previous paper, as shown in Table 1 [7]. The estimated values for $x = 0.5$ are also nearly the same.

In the high-temperature region, considering the previous results for $\chi_{3d\,orb}$, $\chi_{5d\,orb} + (2/3)\,\chi_{Pauli} + \chi_{dia}$ and $y > 0.66$ or $y > 0.73$ in Table 1, we assume $x = 0.2$ and $y = 0.7$ or 0.8. Here, we use $N(\varepsilon_F) = 1.84$ states with (eV)$^{-1}$/V spin estimated in [7] and $N(\varepsilon_F) = 0.91$ states

(eV)$^{-1}$/V spin reported by a band calculation [12]. The obtained values of $K_{3d\,orb}$, $\chi_{3d\,orb}$ and $\chi_{5d\,orb} + (2/3)\,\chi_{Pauli} + \chi_{dia}$ from the K-χ plot are listed in Table 2. The obtained $K_{3d\,orb} = 0.84 \sim 0.87\%$, $\chi_{3d\,orb} = (4.4 \sim 4.5) \cdot 10^{-4}$ emu/mol and $\chi_{5d\,orb} + (2/3)\,\chi_{Pauli} + \chi_{dia} = (0.61 \sim 0.89) \cdot 10^{-4}$ emu/mol are consistent with those obtained in [7] (Table 1). The values $y = 0.7$ or 0.8, and $N(\varepsilon_F) = 1.84$ states (eV)$^{-1}$/V spin or $N(\varepsilon_F) = 0.91$ states (eV)$^{-1}$/V spin do not make so much difference. Therefore, the assumption $x = 0.2$ is considered to be reasonable. In Fig. 2, the parameters, $K_{3d\,orb}$, χ_{orb} and $\chi_{dia} + (2/3)\,\chi_{Pauli}$ for $x = 0.39$ and $y = 0.68$ in the low-temperature region, and for $x = 0.2$, $y = 0.8$ and $N(\varepsilon_F) = 1.84$ states (eV)$^{-1}$/V spin in the high-temperature region are illustrated by broken and solid lines, respectively.

Both below and above T_L, the physical quantities obtained from the K-χ plot are consistent with those estimated in [7]. The change in $N(\varepsilon_F)$, $N_{3d}(\varepsilon_F)$, $K_{3d\,orb}$, $\chi_{3d\,orb}$ and $\chi_{5d\,orb} + (2/3)\,\chi_{Pauli} + \chi_{dia}$ at T_L originates from the lattice transformation.

3. Anisotropy of the Superconducting Energy Gap

In the superconducting state, the low temperature limiting value of K after the diamagnetic correction is larger than $K_{3d\,orb} = 0.66\%$, which is estimated in the low-temperature region in the normal state [7]. This is interpreted as the loss of all of 3d spin susceptibility and means that the Cooper pair is of spin singlet. $1/T_1$ shows a very small enhancement just below T_c, and a T^5 dependence well below T_c, while the electronic specific heat is proportional to T^3 at low temperatures [7, 8]. These temperature dependences mean that the Cooper pair is of a d wave ABM type in which the superconducting energy gap vanishes at points on the Fermi surface.

As a simple example of an even parity d wave ABM gap, the θ- and φ-dependent gap in k-space, $\Delta(\theta, \varphi)$ is written as [13],

$$\Delta(\theta,\varphi) = \frac{1}{2}\,\Delta_0\,[(3\cos^2\theta - 1) + \sqrt{3}\,i\sin^2\theta\sin 2\varphi]. \tag{4}$$

One can ascertain that $|\Delta(\theta, \varphi)|$ vanishes at points, $(\theta, \varphi) = (\theta_1, n\pi/2)$, where $\cos^2\theta_1 = 1/3$ and n is an integer. For another example for the d wave ABM gap, there is an even parity d γ wave,

$$\Delta(\boldsymbol{k}) = \frac{(\cos k_x + \cos k_y - 2\cos k_z)}{\sqrt{6}} \pm i\,\frac{(\cos k_x - \cos k_y)}{\sqrt{2}}, \tag{5}$$

or an even parity d ε wave,

$$\Delta(\boldsymbol{k}) = \sin(k_x)\sin(k_y) + \varepsilon\sin(k_y)\sin(k_z) + \varepsilon^2\sin(k_z)\sin(k_x), \tag{6}$$

gap in the respective coordinate, where $\varepsilon = (-1 + i\sqrt{3})/2$. There are nodes in the [1, 1, 1] and equivalent directions on the Fermi surface both in the d γ and d ε energy gaps.

The ratio $(1/T_1)_s/(1/T_1)_n$ of the spin-lattice relaxation rate $(1/T_1)_s$ in the superconducting state to $(1/T_1)_n$ in the normal state at the same temperature T is written in the form [14]

$$\frac{(1/T_1)_s}{(1/T_1)_n} = \frac{2}{k_B T}\int_0^\infty dE\,[N_s^2(E) + M_s^2(E)] \cdot f(E)(1 - f(E)), \tag{7}$$

where $f(E)$ is the Fermi-Dirac distribution function, $N_s(E)$ DOS in the superconducting state and $M_s(E)$ the coherent factor term. $N_s(E)$ and $M_s(E)$ are written as

$$N_s(E) = \frac{E}{4\pi}\int d\Omega\,\frac{1}{\sqrt{E^2 - \Delta^2(\theta,\varphi)}}, \tag{8}$$

$$M_s(E) = \frac{1}{4\pi}\int d\Omega\,\frac{\Delta(\theta,\varphi)}{\sqrt{E^2 - \Delta^2(\theta,\varphi)}}. \tag{9}$$

$M_s(E)$ is caused by the following processes. When the Cooper pair is of spin singlet, the interactions $H_{IS}^{+} = A\sum_{k,k'} I_+\,a_{k',\downarrow}^*\,a_{k',\uparrow}$ and $H_{IS}^{-} = A\sum_{k,k'} I_-\,a_{k',\uparrow}^*\,a_{k',\downarrow}$, which bring about the spin-lattice relaxation, induce the transition between the following electronic states: initial state $|i\rangle$ with an electron with wave vector $\boldsymbol{k}$ and spin $\uparrow$, and a Cooper pair $(\boldsymbol{k}', \uparrow, -\boldsymbol{k}', \downarrow)$, and final state $|f\rangle$ with an electron with wave vector $-\boldsymbol{k}'$ and spin $\downarrow$, and a Cooper pair $(\boldsymbol{k}', \uparrow, -\boldsymbol{k}', \downarrow)$. $|i\rangle$ and $|f\rangle$ are written in terms of the creation and annihilation operators $a_{k\sigma}^*$ and $a_{k\sigma}$ of the conduction electron with wave vector $\boldsymbol{k}$ and spin σ as

$$|i\rangle = [(1 - h_{k'})^{1/2} + h_{k'}^{1/2}\,a_{k'\uparrow}^*\,a_{-k'\downarrow}^*]\,a_{k'\uparrow}^*\,|0\rangle, \tag{10}$$

$$|f\rangle = [(1 - h_k)^{1/2} + h_k^{1/2}\,a_{k\uparrow}^*\,a_{-k\downarrow}^*]\,a_{-k'\downarrow}^*\,|0\rangle, \tag{11}$$

where $|0\rangle$ is a vacuum state and

$$h_k = \frac{1}{2}\left(1 - \frac{\varepsilon_k}{E_k}\right), \tag{12}$$

where $\varepsilon_{\boldsymbol{k}}$ is the energy of an electron with wave vector $\boldsymbol{k}$ measured from the Fermi energy and $E_{\boldsymbol{k}} = \sqrt{\varepsilon_{\boldsymbol{k}}^2 + \Delta^2(\theta, \varphi)}$. $(1/T_1)_s$ is proportional to the square of the matrix element $\langle f \,|\, H_{IS}^{+} \,|\, i \rangle$. Substituting (10) and (11), $(1/T_1)_s$ is proportional to $[(1 - h_{\boldsymbol{k}})^{1/2} (1 - h_{\boldsymbol{k}'})^{1/2} + h_{\boldsymbol{k}}^{1/2} h_{\boldsymbol{k}'}^{1/2}]^2$.

$$\left(\frac{1}{T_1}\right)_s \propto \int \mathrm{d}E \int \mathrm{d}E' \int \mathrm{d}\Omega \int \mathrm{d}\Omega' \cdot \frac{(EE' + \Delta\Delta')}{\sqrt{E^2 - \Delta^2}\,\sqrt{E'^2 - \Delta'^2}} \cdot f(E)\,(1 - f(E'))\,\delta(E - E'). \tag{13}$$

$M_s(E)$ comes from the second term in (13).

In the case of a spin triplet Cooper pair, we have to consider the transition between the following electronic states instead of (10) and (11):

$$|i\rangle = [(1 - h_{\boldsymbol{k}'})^{1/2} + h_{\boldsymbol{k}'}^{1/2}\, a_{\boldsymbol{k}'\uparrow}^{*}\, a_{-\boldsymbol{k}'\uparrow}^{*}]\, a_{\boldsymbol{k}\uparrow}^{*} |0\rangle, \tag{14}$$

$$|f\rangle = [(1 - h_{\boldsymbol{k}})^{1/2} + h_{\boldsymbol{k}}^{1/2}\, a_{\boldsymbol{k}\uparrow}^{*}\, a_{-\boldsymbol{k}\uparrow}^{*}]\, a_{-\boldsymbol{k}'\downarrow}^{*} |0\rangle. \tag{15}$$

In this case, $|\langle f \,|\, H_{IS}^{+} \,|\, i \rangle|^2$ is proportional to $(1 - h_{\boldsymbol{k}})(1 - h_{\boldsymbol{k}'})$.

$$\left(\frac{1}{T_1}\right)_s \propto \int \mathrm{d}E \int \mathrm{d}E' \int \mathrm{d}\Omega \int \mathrm{d}\Omega' \cdot \frac{EE'}{\sqrt{E^2 - \Delta^2}\,\sqrt{E'^2 - \Delta'^2}} \cdot f(E)\,(1 - f(E'))\,\delta(E - E'), \tag{16}$$

and $M_s(E)$ disappears.

In case of anisotropy expressed by (4) one can ascertain the relation

$$\int \mathrm{d}\Omega\, \Delta(\theta, \varphi) = 0. \tag{17}$$

Because the denominator of the integrand in (9) contains $\Delta(\theta, \varphi)$, (17) does not mean that $M_s(E) = 0$ directly. To ascertain whether $M_s(E) = 0$ or not, we carried out a numerical calculation of (9) and found that $M_s(E)$ is at most 10^{-2} and negligibly small compared to $N_s(E)$. Without the calculation of the temperature dependence of $(1/T_1)_s$ according to (7), it is not clear whether d wave gaps expressed by (4)–(6) are really appropriate for HfV_2. The calculation of $(1/T_1)_s$ with these ABM gaps is now in progress.

4. Summary

We have investigated the change in the electronic state in the C15 Laves phase compound HfV_2 above and below the lattice transformation temperature T_L by a K-χ plot. Both below and above T_L, the physical quantities obtained from the K-χ plot are consistent with those estimated in [7]. The change in $N(\varepsilon_F)$, $N_{3d}(\varepsilon_F)$, $K_{3d\,orb}$, $\chi_{3d\,orb}$ and $\chi_{5d\,orb} + (2/3)\,\chi_{Pauli} + \chi_{dia}$ at T_L originates from the lattice transformation.

In the superconducting state, we discussed the d wave ABM type energy gap in which the gap vanishes at points on the Fermi surface.

[1] H. Kotegawa, K. Ishida, Y. Kitaoka, T. Muranaka, and J. Akimitsu, Phys. Rev. Lett. **87,** 127001 (2001).
[2] K. Ishida, H. Mukuda, Y. Kitaoka, Z. Q. Mao, Y. Mori, and Y. Maeno, Phys. Rev. Lett. **84,** 5387 (2001).
[3] T. Mito, S. Kawasaki, G.-q. Zheng, Y. Kawasaki, K. Ishida, Y. Kitaoka, D. Aoki, Y. Haga, and Y. Onuki, Phys. Rev. B **63,** 220507(R) (2001).
[4] Y. Kohori, Y. Yamato, Y. Iwamoto, T. Kohara, E. D. Bauer, M. B. Maple, and J. L. Sarrao, Phys. Rev. B **64,** 134526 (2001).
[5] P. W. Anderson and C. C. Yu, Highlights of Condensed Matter Theory, ed. F. Bassani, F. Fumi, and M. P. Tosi, North-Holland, Amsterdam 1985, p. 767.
[6] T. Matsuura and K. Miyake, J. Phys. Soc. Japan **55,** 29 (1986); **55,** 610 (1986).
[7] Y. Kishimoto, T. Ohno, T. Hihara, K. Sumiyama, and K. Suzuki, Phys. Rev. B **64,** 024509 (2001).
[8] Y. Kishimoto, N. Shibata, T. Ohno, Y. Kitaoka, K. Asayama, K. Amaya, and T. Kanashiro, J. Phys. Soc. Japan **61,** 696 (1992).
[9] A. M. Clogston, A. G. Gossard, V. Jaccarino, and Y. Yafet, Phys. Rev. Lett. **9,** 262 (1962).
[10] R. R. Gupta, Landolt-Börnstein ed. O. Madelung, Springer-Verlag, Berlin 1986; Group II, Vol. 16, p. 402.
[11] A. J. Freeman and R. E. Watson, Magnetism II A, ed. G. T. Rado and H. Suhl, Academic Press, New York 1965, p. 165.
[12] A. Ormeci, F. Chu, J. M. Wills, T. E. Mitchel, R. C. Albers, D. J. Thoma, and S. P. Chen. Phys. Rev. B **54,** 12753 (1996).
[13] P. W. Anderson and P. Morel, Phys. Rev. **123,** 1911 (1961).
[14] D. E. Maclaughlin, Solid State Physics, ed. H. Ehrenreigh, F. Seitz, and D. Turnbull, Academic Press, New York 1973, Vol. **32,** 1 (1976).